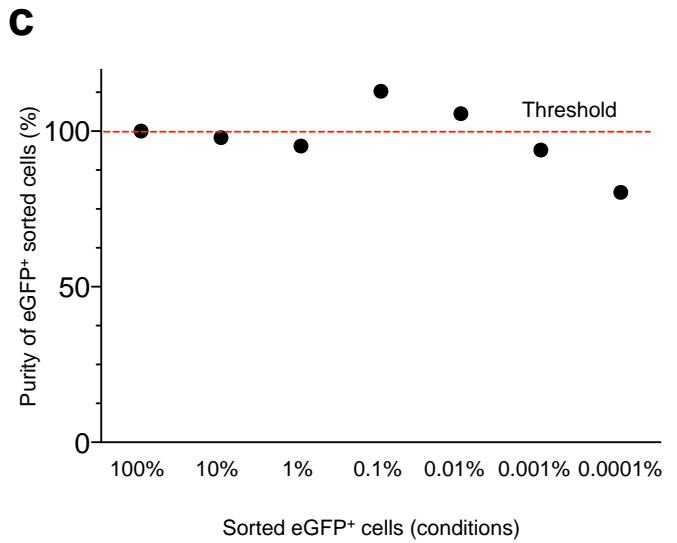
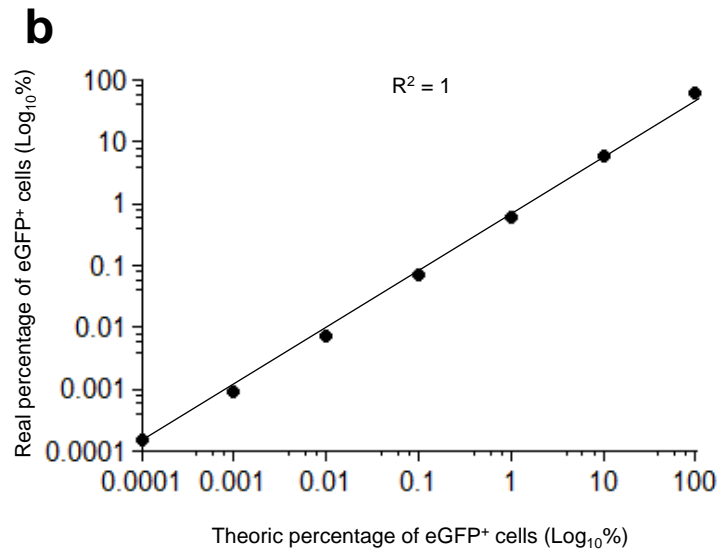
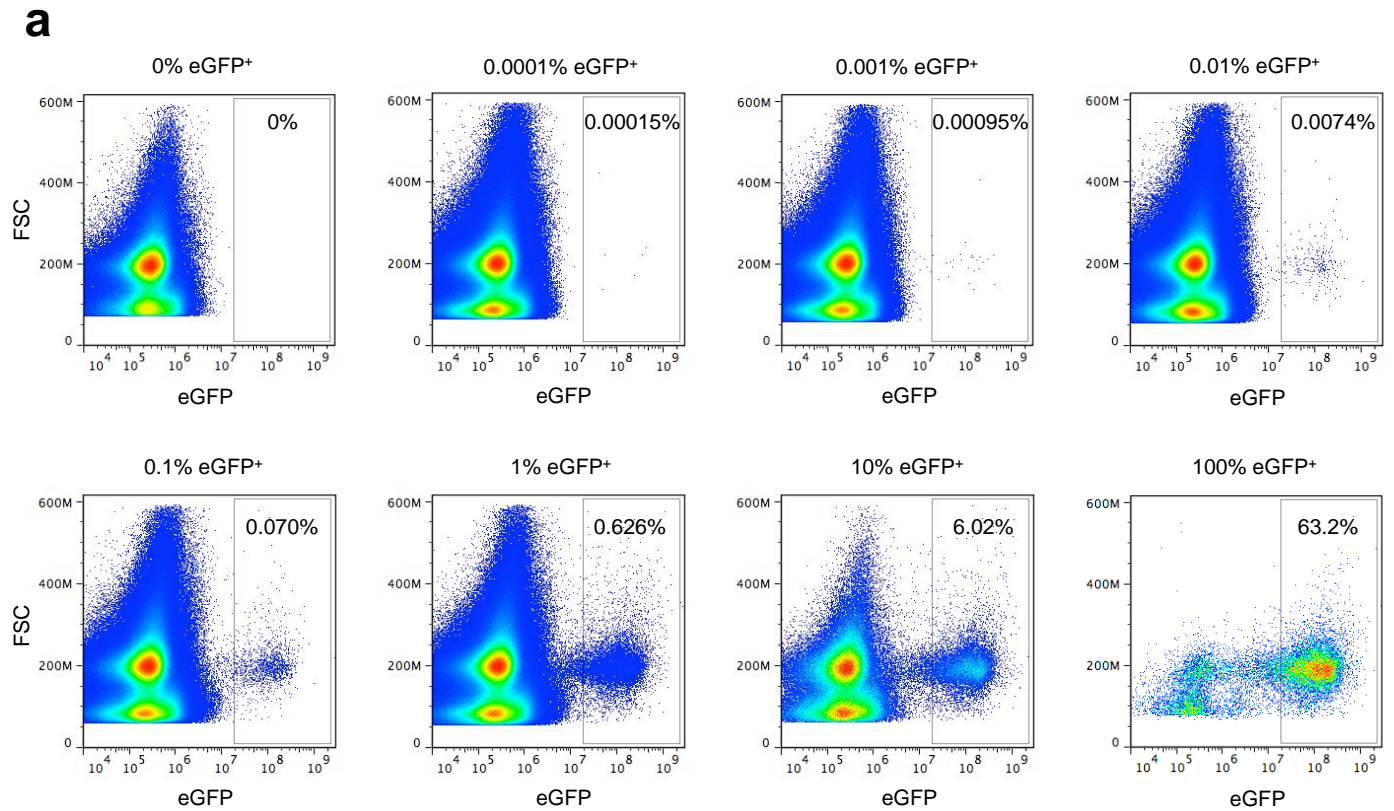


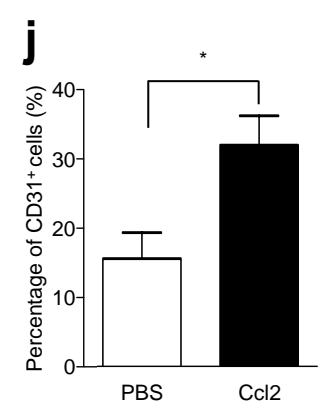
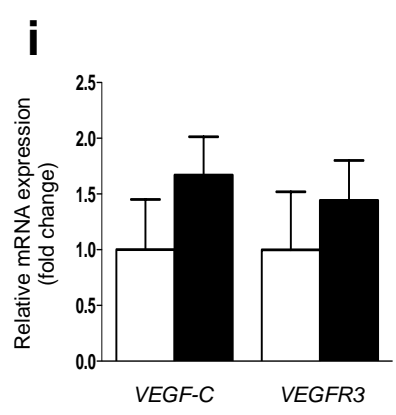
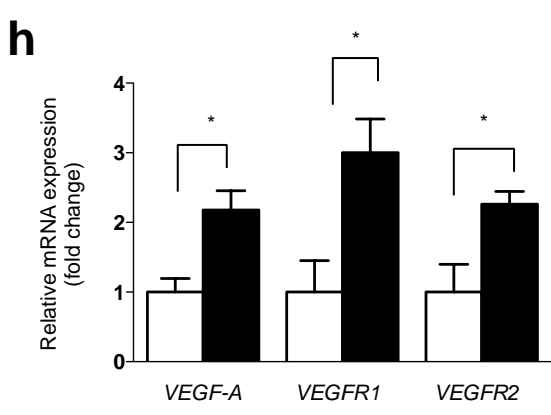
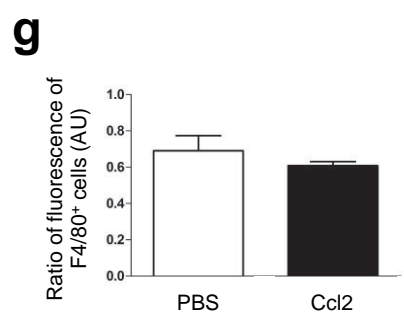
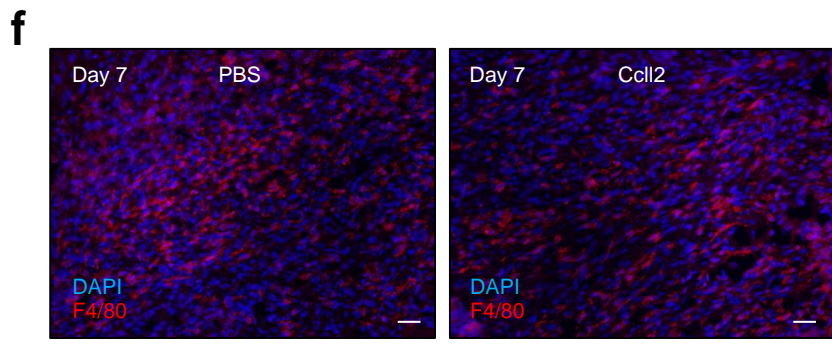
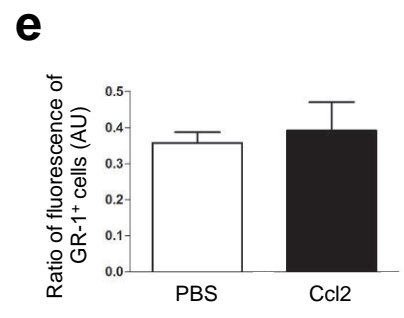
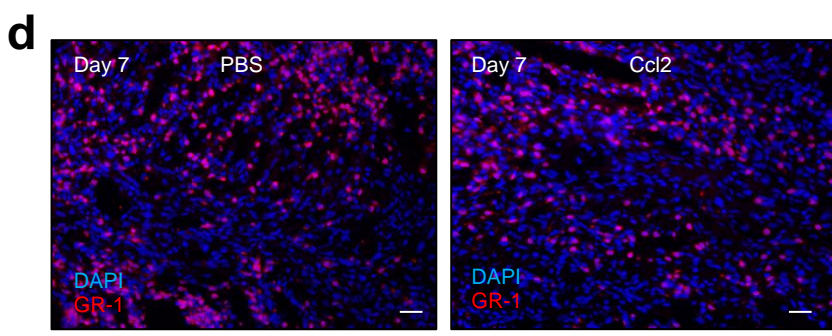
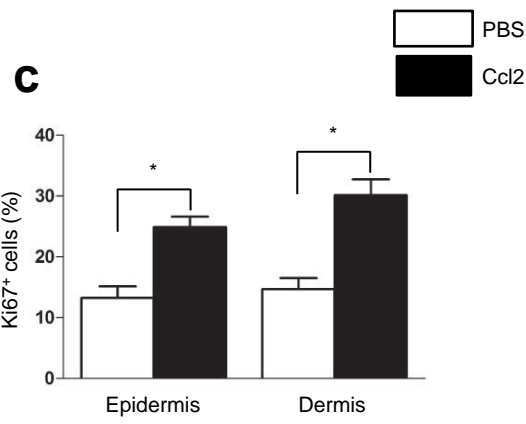
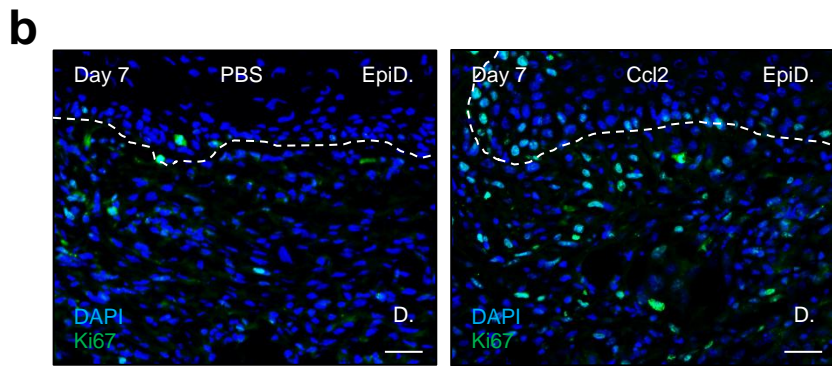
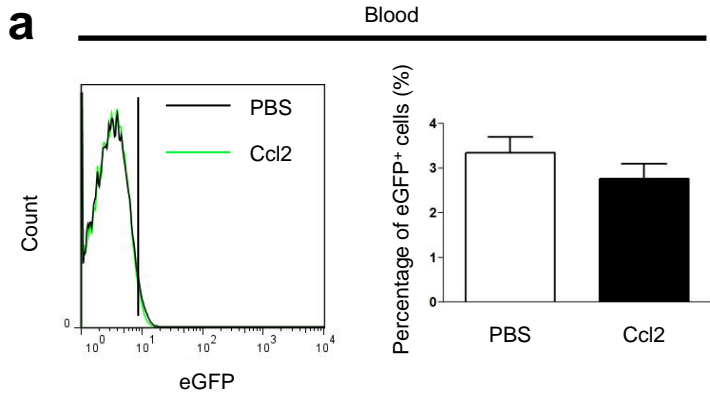
Supplementary Figure 1: Experimental design

WT females are mated with eGFP males. On embryonic day 15.5, surgical wounds are done on the back of the pregnant mice. Mice are sacrificed at days 1 to 9 post wounding. Blood, bone marrow and skin wounds were harvested and analyzed.



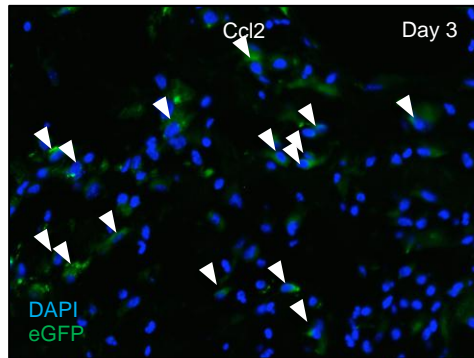
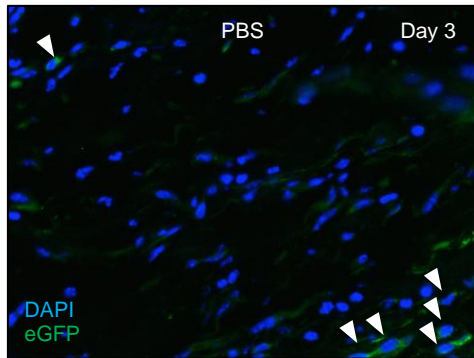
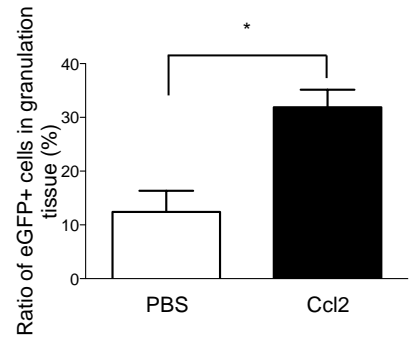
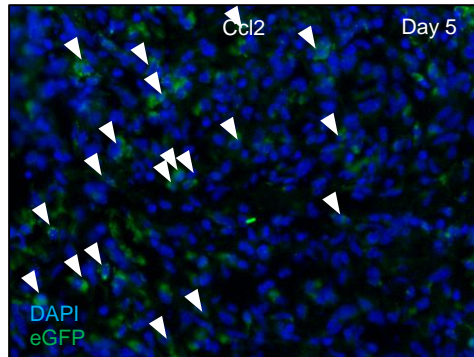
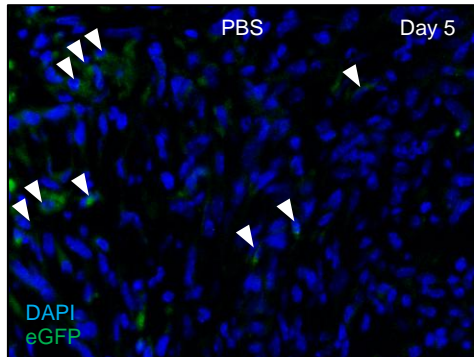
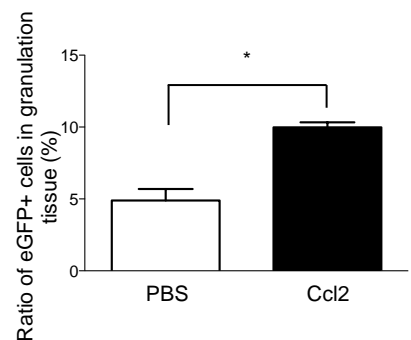
Supplementary Figure 2: Efficiency of eGFP⁺ cells FACS detection

Spleen from WT and eGFP mice were disrupted and put in cell suspension (a) Representative FACS results of eGFP⁺ cells diluted in WT cells from 100% to 0.0001%. Each plot shows 2 millions events. (b) Linear regression of FACS analysis. (c) qPCR on genomic DNA from sorted eGFP⁺ cells.



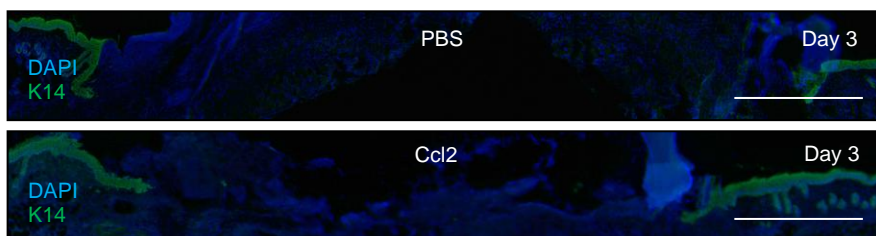
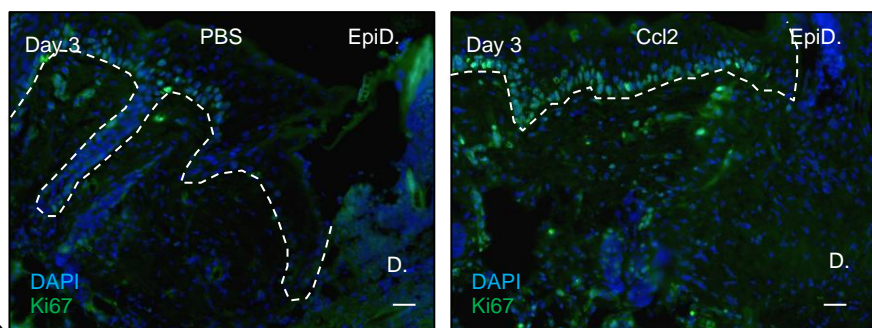
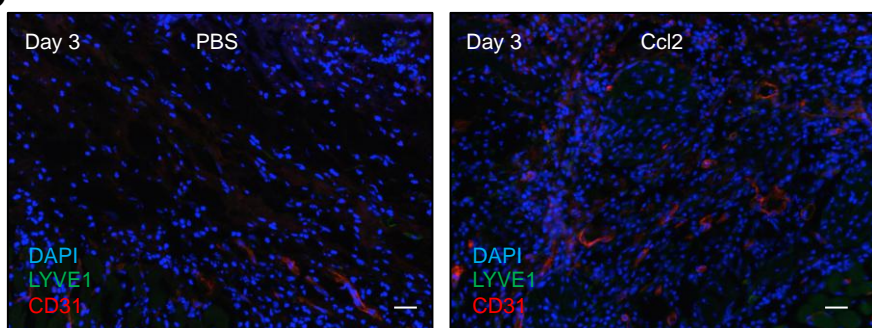
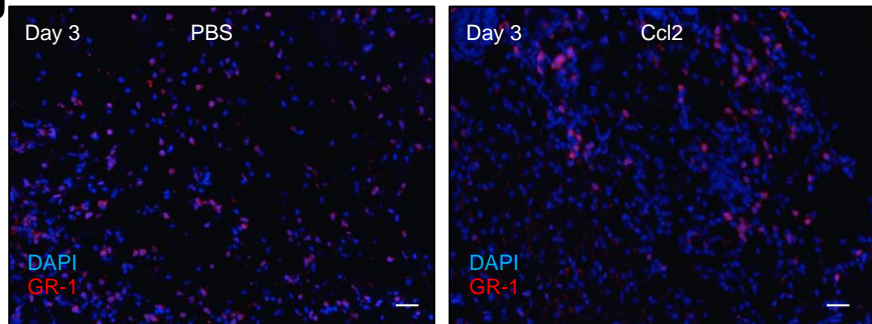
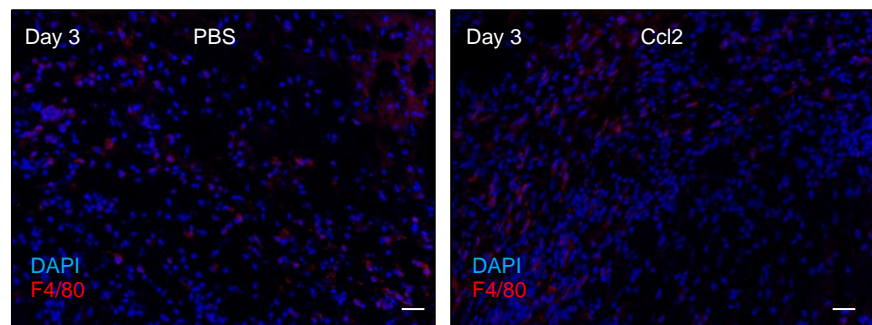
Supplementary Figure 3: Ccl2 administration enhance maternal angiogenesis

(a) Representative FACS analysis and quantification of eGFP⁺ cells in the blood on day 7 after wounding, in pregnant mice carrying eGFP⁺ fetuses receiving injections of PBS (black line) or Ccl2 (green line) into the wound ($n = 3$). (b) Labeling for Ki67 (green) in the wound on day 7. Scale bars: 50 μ m. (c) Quantification of Ki67⁺ cells in epidermal wound edges (EpiD) and the dermal granulation tissues (D) ($n = 4$). (d) Labeling of the wound for GR-1 (red). Scale bars: 50 μ m. (e) Quantification of GR-1⁺ cells by fluorescence densitometry on granulation tissue on day 7 ($n = 4$). (f) Labeling of the wound for F4/80 (red). Scale bars: 50 μ m. (g) Quantification of F4/80⁺ cells by fluorescence densitometry on granulation tissue ($n = 4$). (h) Quantitative RT-PCR analysis of *VEGF-A*, *VEGFR1*, and *VEGFR2* mRNA levels normalized against *Gapdh* mRNA levels in the wound ($n = 5$). (i) Quantitative RT-PCR analysis of *VEGF-C* and *VEGFR3* mRNA levels normalized against *Gapdh* mRNA levels in the wound ($n = 5$). (j) FACS analysis showed that there were significantly larger numbers of CD31⁺ cells in the wounds of pregnant mice treated with Ccl2 than in those treated with PBS ($n = 3$). Student's *t*-test, * $p < 0.05$; mean \pm SEM.

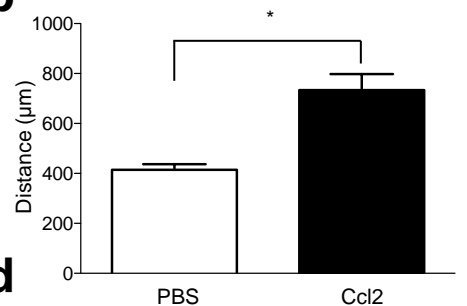
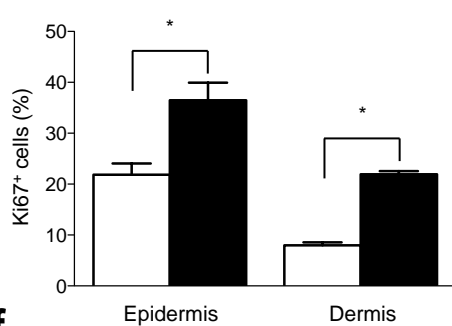
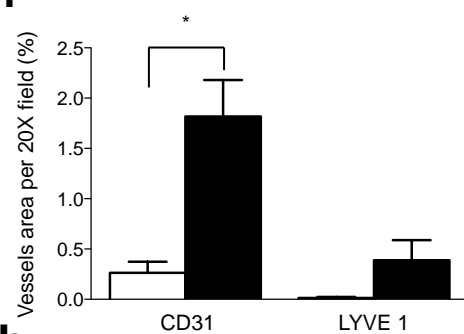
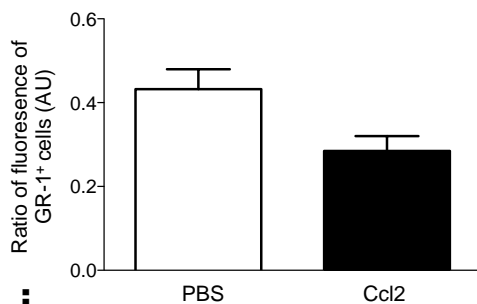
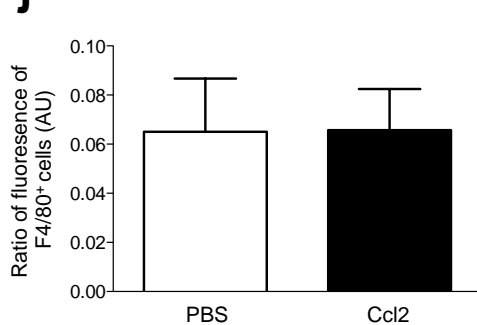
a**b****c****d**

Supplementary Figure 4: Ccl2 recruits FMCs to maternal wounds early during healing process

An 8 mm wound was created in pregnant female mice carrying eGFP⁺ fetuses. We injected PBS or Ccl2 into the wound immediately and two days after skin excision. **(a and c)** Representative micrographs of the spontaneous fluorescence of eGFP⁺ (green) cells in granulation tissue, indicated by white arrowheads. **(b and d)** Quantifications of eGFP⁺ cells in sections of wounds from pregnant mice carrying eGFP⁺ fetuses after the injections of PBS or Ccl2 ($n = 3$)

a**c****e****g****i**

 PBS
 Ccl2

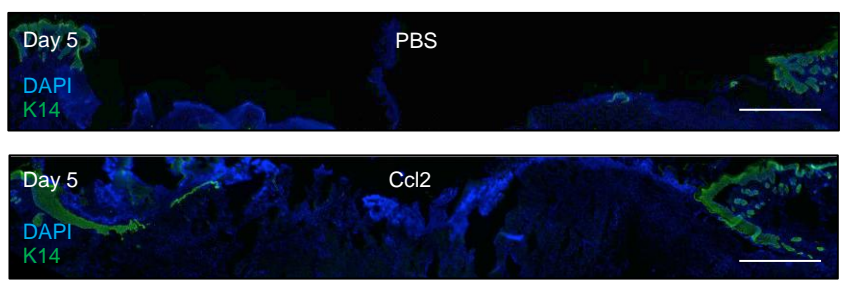
b**d****f****h****j**

Supplementary Figure 5: Ccl2 recruits FMCs to maternal wounds and improve at day 3 skin wound healing in pregnant mice

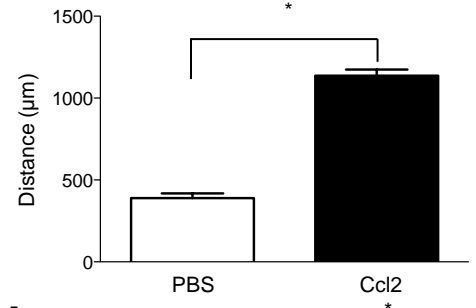
An 8 mm wound was created in pregnant female mice carrying eGFP⁺ fetuses. We injected PBS or Ccl2 into the wound immediately and two days after skin excision. **(a)** Anti-K14 (green) labeling of neoepidermal tongues in the wound. Scale bars: 1mm **(b)** Measurement of neoepidermal tongues at wound sites ($n = 3$). **(c)** Anti-Ki67 (green) labeling of the wound. Scale bars: 50 μ m. **(d)** Quantification of Ki67⁺ cells in epidermal wound edges (EpiD) and the dermal granulation tissues (D) ($n = 3$). **(e)** Dual labeling for CD31 (red) and LYVE1 (green). Scale bars: 50 μ m. **(f)** Quantification of relative vessel area per 20x field by fluorescence densitometry ($n = 3$). **(g)** Labeling of the wound for GR-1 (red). Scale bars: 50 μ m. **(h)** Quantification of GR-1⁺ cells by fluorescence densitometry on granulation tissue on day 3 ($n = 3$). **(i)** Labeling of the wound for F4/80 (red). Scale bars: 50 μ m. **(j)** Quantification of F4/80⁺ cells by fluorescence densitometry on granulation tissue ($n = 3$).

PBS
 Ccl2

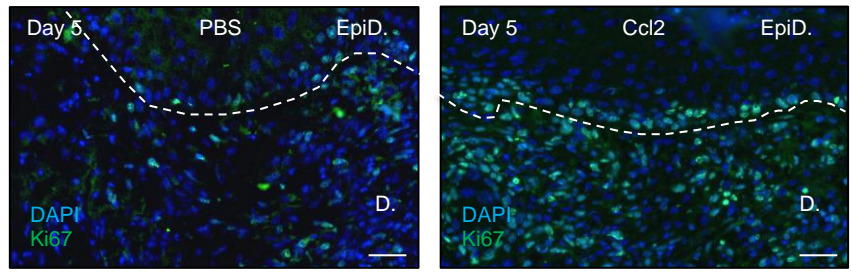
a



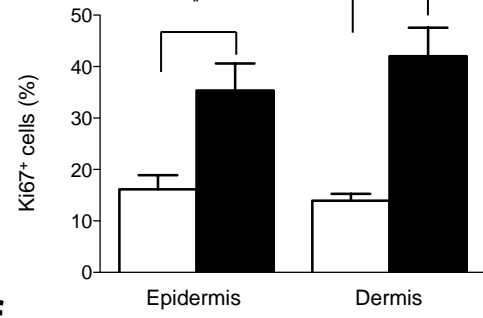
b



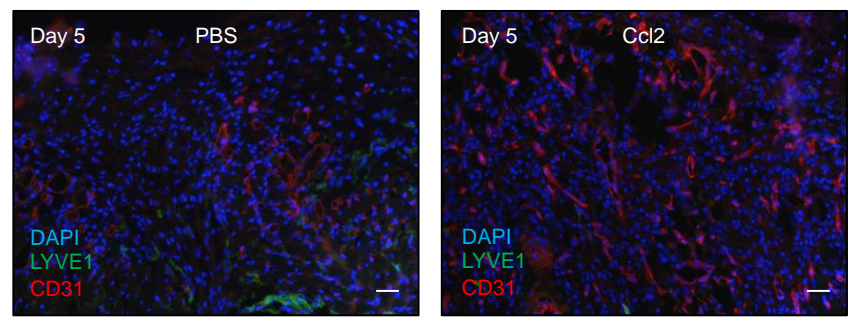
c



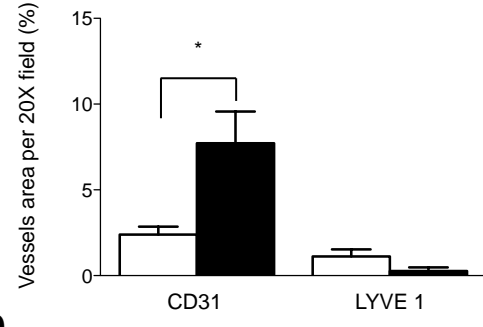
d



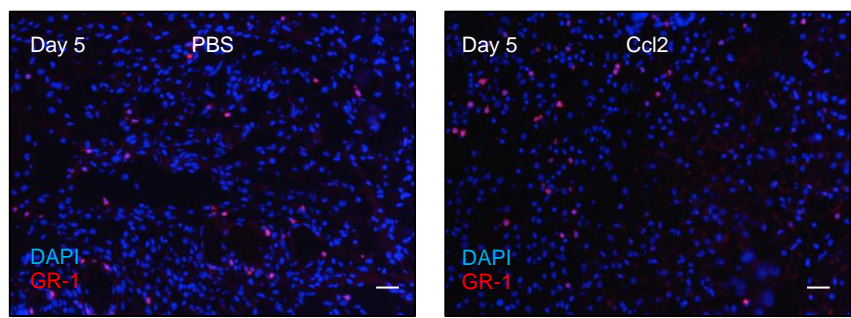
e



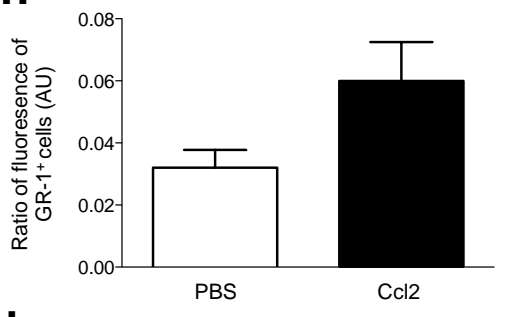
f



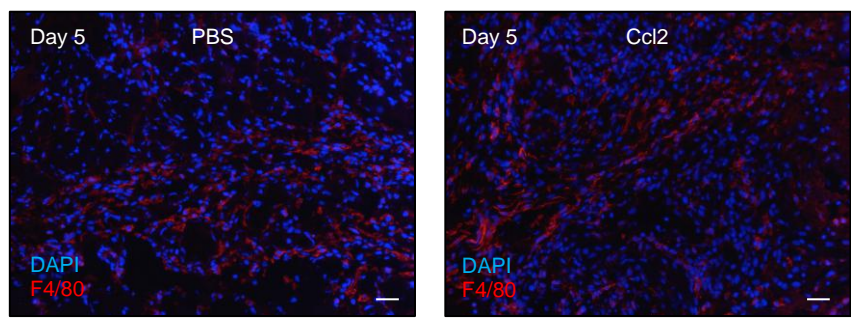
g



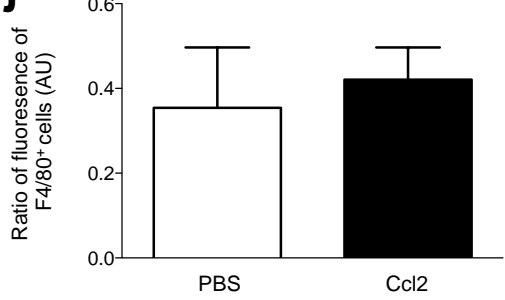
h



i

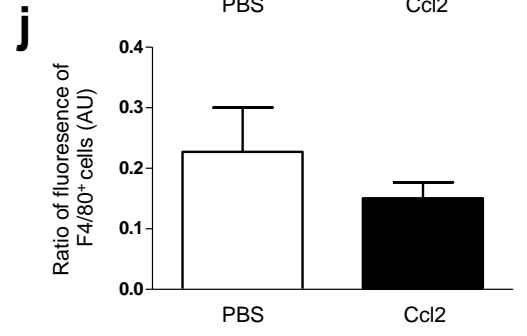
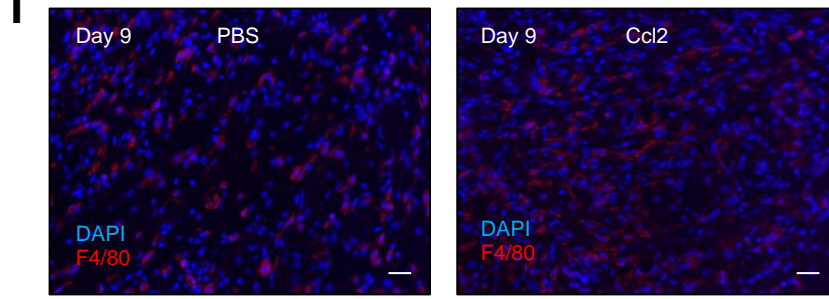
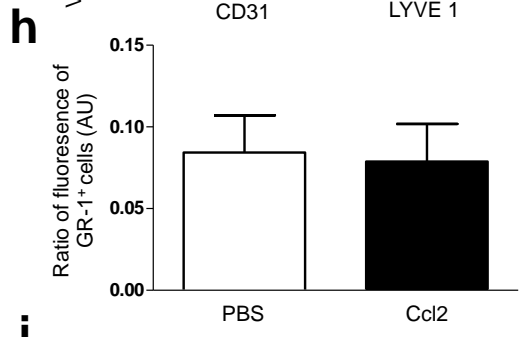
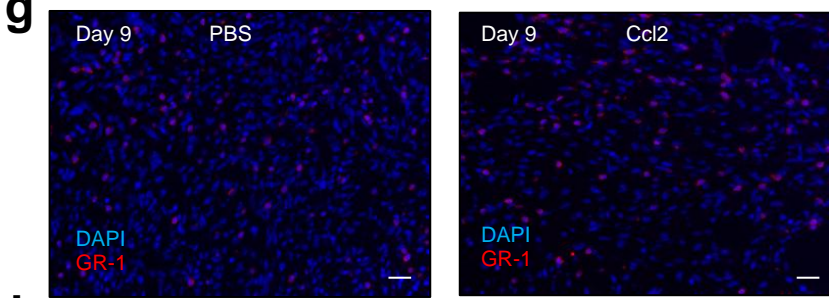
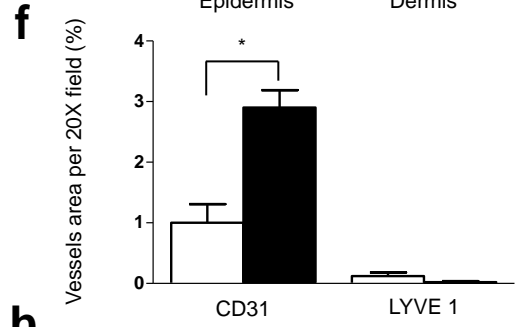
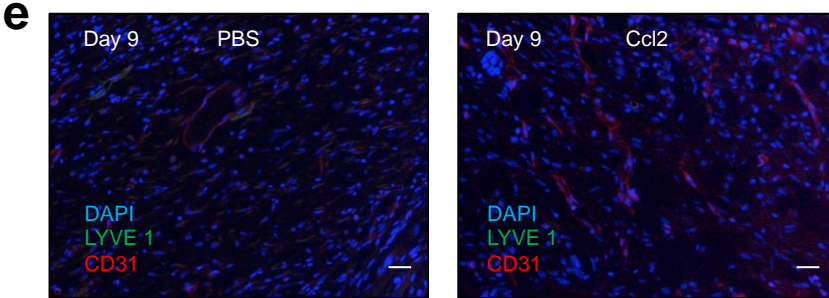
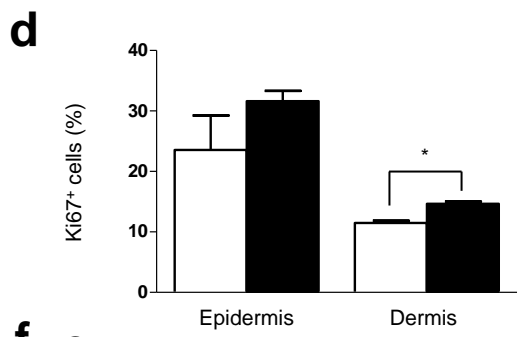
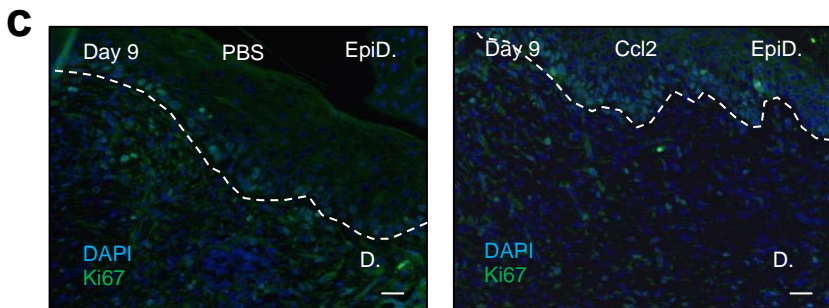
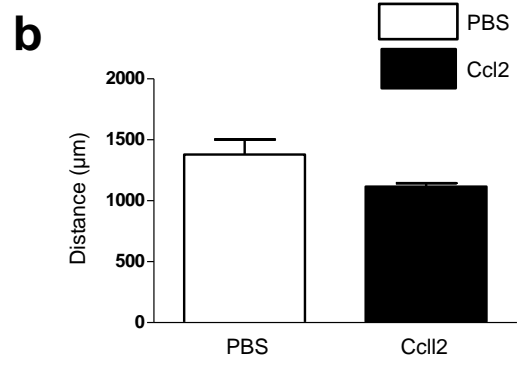
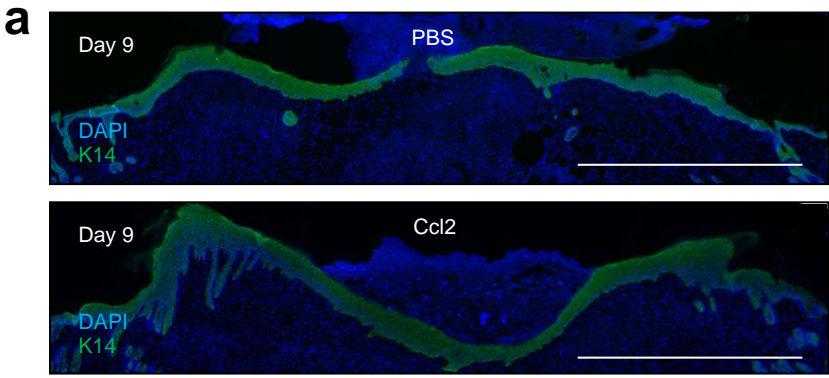


j



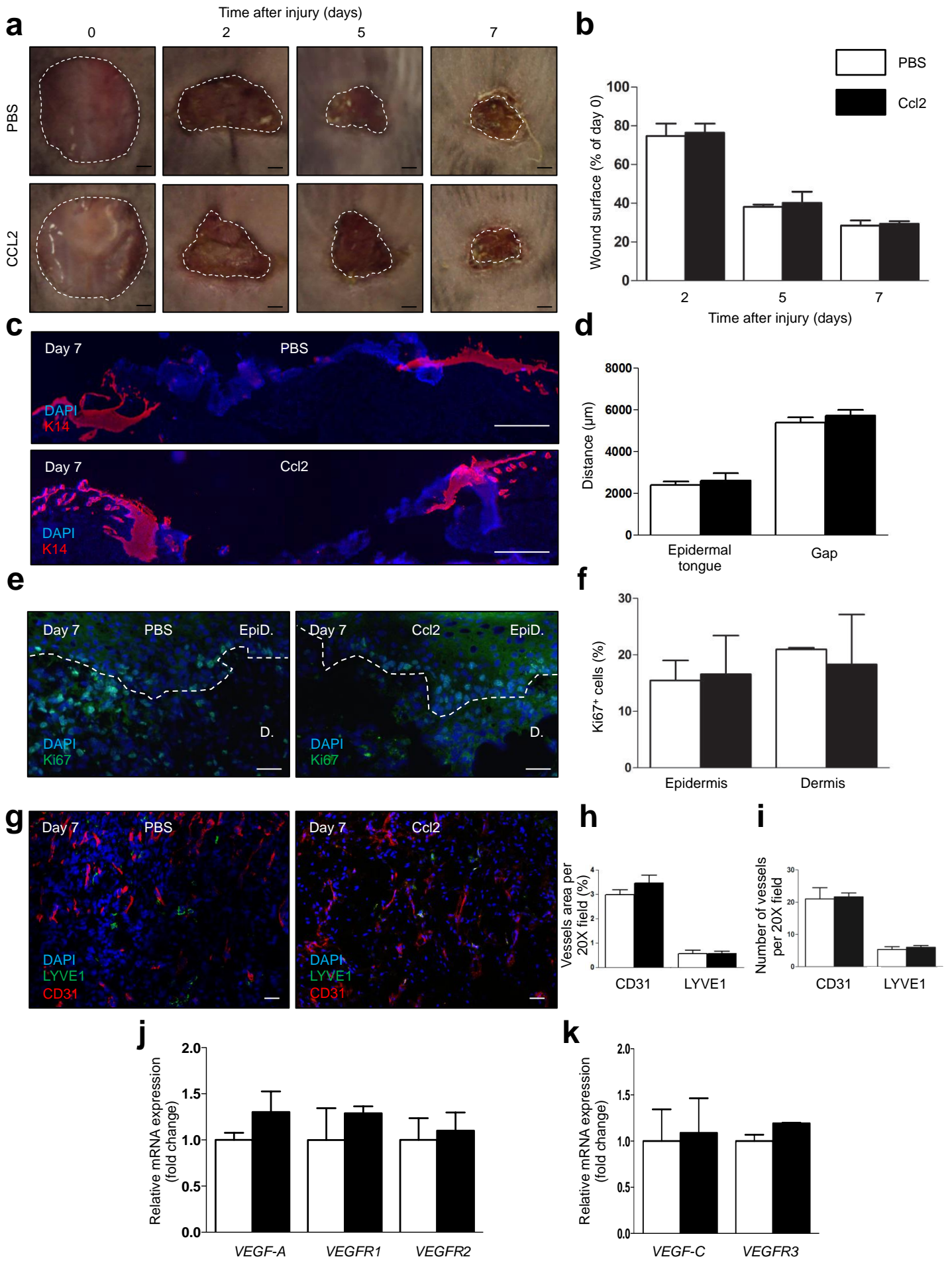
Supplementary Figure 6: Ccl2 recruits FMCs to maternal wounds and improve at day 5 skin wound healing in pregnant mice

An 8 mm wound was created in pregnant female mice carrying eGFP⁺ fetuses. We injected PBS or Ccl2 into the wound immediately and two days after skin excision. **(a)** Anti-K14 (green) labeling of neoepidermal tongues in the wound. Scale bars: 1mm **(b)** Measurement of neoepidermal tongues at wound sites ($n = 3$). **(c)** Anti-Ki67 (green) labeling of the wound. Scale bars: 50 μ m. **(d)** Quantification of Ki67⁺ cells in epidermal wound edges (EpiD) and the dermal granulation tissues (D) ($n = 3$). **(e)** Dual labeling for CD31 (red) and LYVE1 (green). Scale bars: 50 μ m. **(f)** Quantification of relative vessel area per 20x field by fluorescence densitometry ($n = 3$). **(g)** Labeling of the wound for GR-1 (red). Scale bars: 50 μ m. **(h)** Quantification of GR-1⁺ cells by fluorescence densitometry on granulation tissue on day 5 ($n = 3$). **(i)** Labeling of the wound for F4/80 (red). Scale bars: 50 μ m. **(j)** Quantification of F4/80⁺ cells by fluorescence densitometry on granulation tissue ($n = 3$).



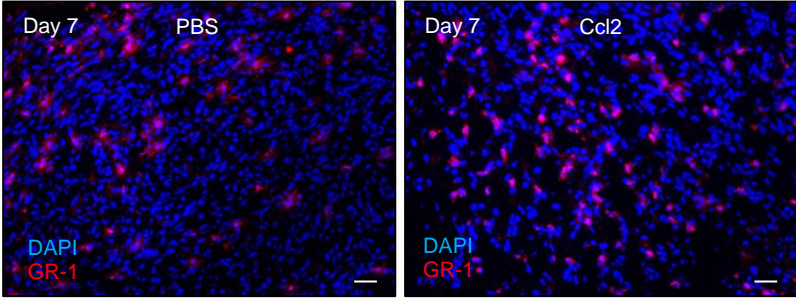
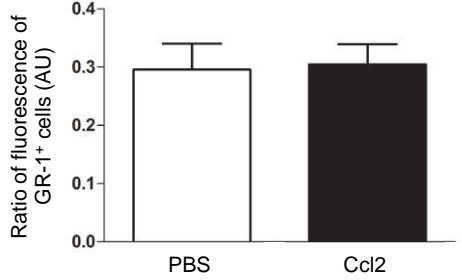
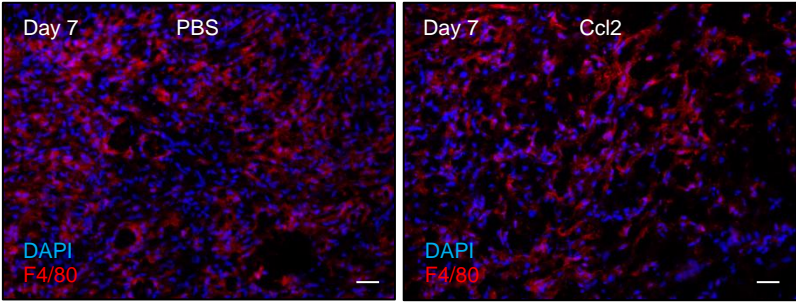
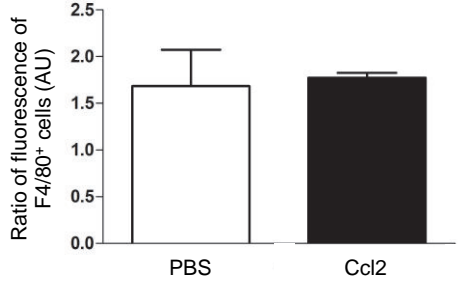
Supplementary Figure 7: Ccl2 recruits FMCs to maternal wounds and improve at day 9 angiogenesis in wound healing in pregnant mice

An 8 mm wound was created in pregnant female mice carrying eGFP⁺ fetuses. We injected PBS or Ccl2 into the wound immediately and two days after skin excision. **(a)** Anti-K14 (green) labeling of neoepidermal tongues in the wound. Scale bars: 1mm **(b)** Measurement of neoepidermal tongues at wound sites ($n = 3$). **(c)** Anti-Ki67 (green) labeling of the wound. Scale bars: 50 μ m. **(d)** Quantification of Ki67⁺ cells in epidermal wound edges (EpiD) and the dermal granulation tissues (D) ($n = 3$). **(e)** Dual labeling for CD31 (red) and LYVE1 (green). Scale bars: 50 μ m. **(f)** Quantification of relative vessel area per 20x field by fluorescence densitometry ($n = 3$). **(g)** Labeling of the wound for GR-1 (red). Scale bars: 50 μ m. **(h)** Quantification of GR-1⁺ cells by fluorescence densitometry on granulation tissue on day 9 ($n = 3$). **(i)** Labeling of the wound for F4/80 (red). Scale bars: 50 μ m. **(j)** Quantification of F4/80⁺ cells by fluorescence densitometry on granulation tissue ($n = 3$).



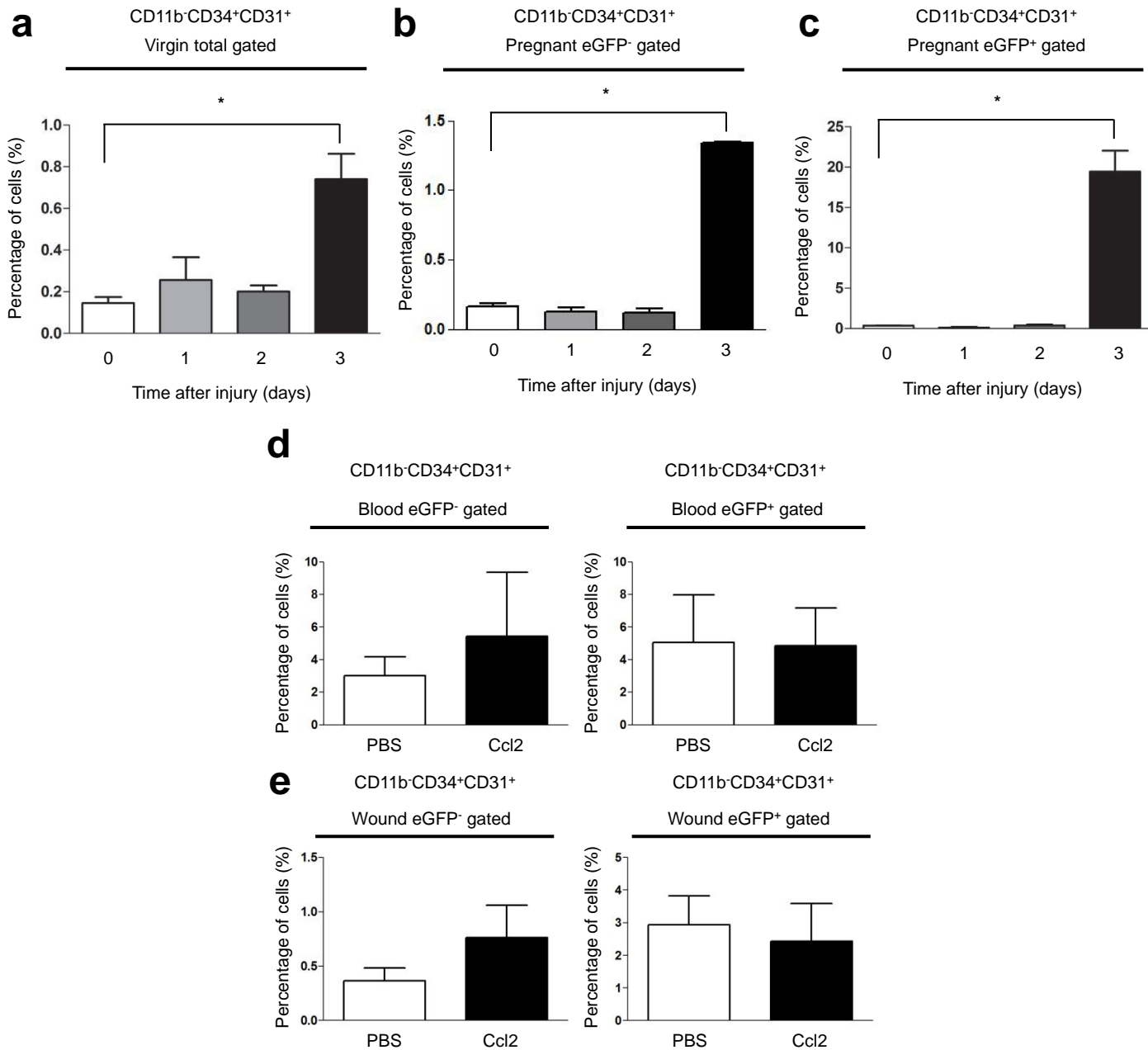
Supplementary Figure 8: CCL2 administration does not affect wound healing in virgin mice

An 8 mm wound was created in virgin female mice and PBS or Ccl2 was injected into the wound immediately and two days after skin excision. **(a)** Time course of skin wound healing. Scale bars: 1mm. **(b)** Planimetry of wound area relative to the original wound area, at various time points ($n = 3$). **(c)** Anti-K14 (red) labeling of neopepidermal tongues and gaps in the wound on day 7. Scale bars: 1mm. **(d)** Measurement of neopepidermal tongues and gaps in the wound ($n = 3$). **(e)** Anti-Ki67 (green) labeling in the wound. Scale bars: 50 μ m. **(f)** Quantification of Ki67⁺ cells in epidermal wound edges (EpiD) and dermal granulation tissues (D) ($n = 3$). **(g)** Dual labeling for CD31 (red) and LYVE1 (green) in the wound. Scale bars: 50 μ m. **(h)** Quantification of relative vessel area per 20x field by fluorescence densitometry ($n = 3$). **(i)** Quantification of the number of vessel types per 20x field ($n = 3$). **(j)** Quantitative RT-PCR analysis of *VEGF-A*, *VEGFR1*, and *VEGFR2* mRNA levels normalized against *Gapdh* mRNA levels in the wound ($n = 3$). **(k)** Quantitative RT-PCR analysis of *VEGF-C* and *VEGFR3* mRNA levels normalized against *Gapdh* mRNA levels in the wound ($n = 3$).

a**b****c****d**

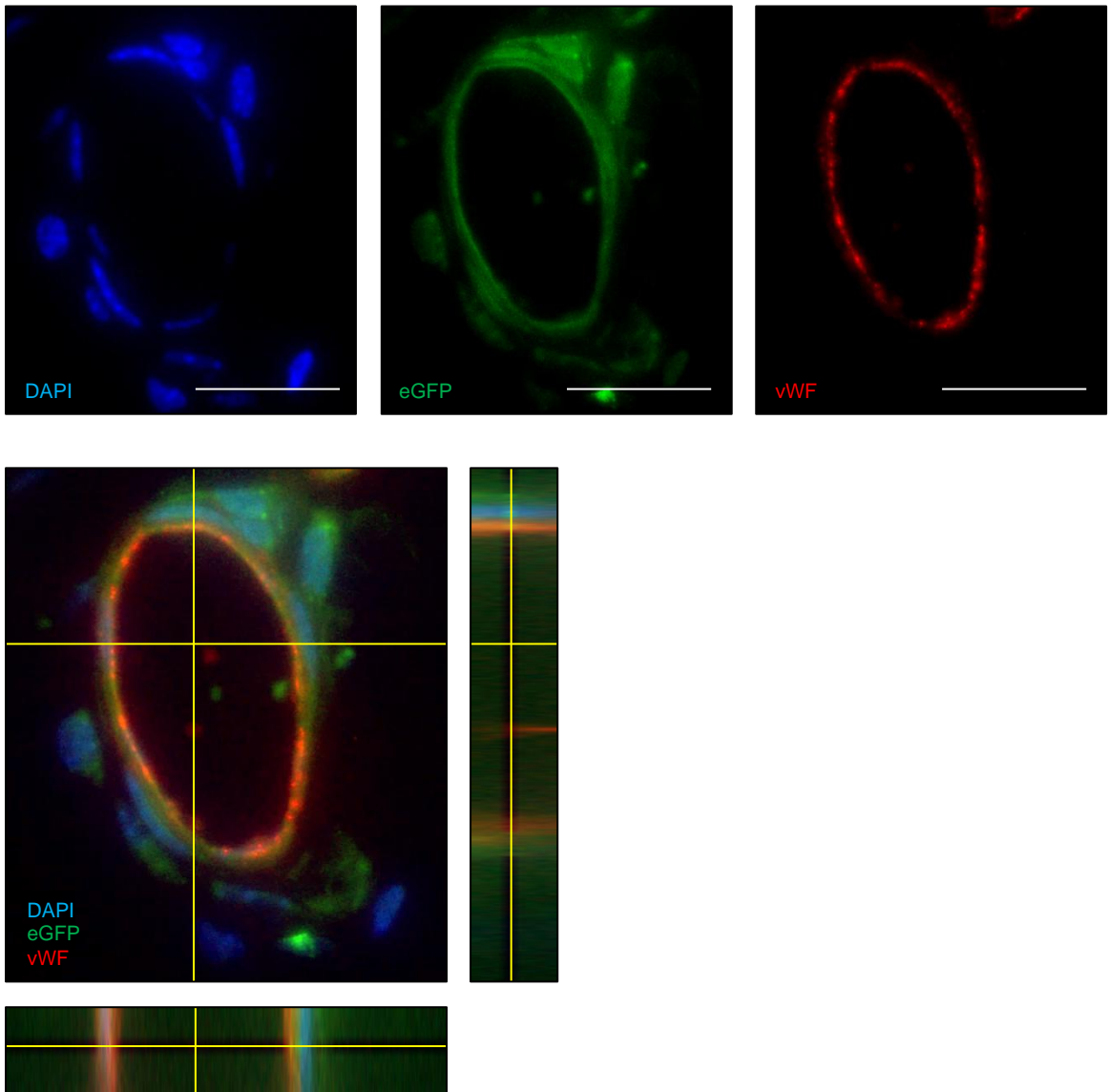
Supplementary Figure 9: Ccl2 administration does not affect inflammation during wound healing in virgin mice

(a) Anti-GR-1 (red) labeling in the wound on day 7. Scale bars: 50 μ m. (b) Quantification of GR-1⁺ cells by fluorescence densitometry on granulation tissue ($n = 3$). (c) Anti-F4/80 (red) labeling of the wound. Scale bars: 50 μ m. (d) Quantification of F4/80⁺ cells by fluorescence densitometry on granulation tissue ($n = 3$).



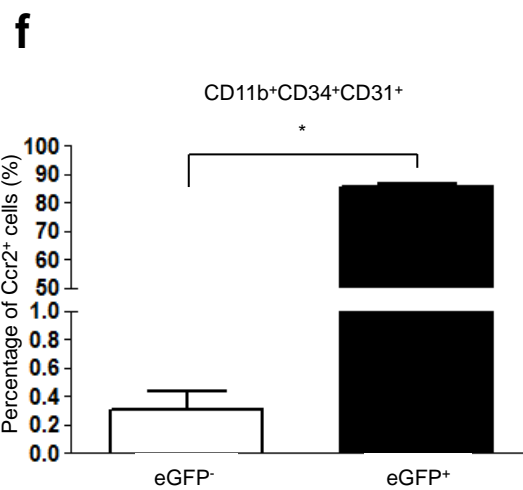
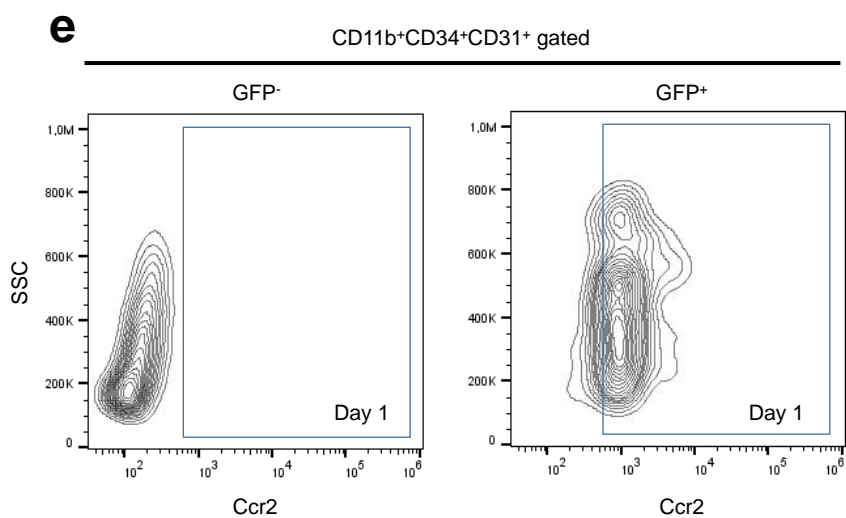
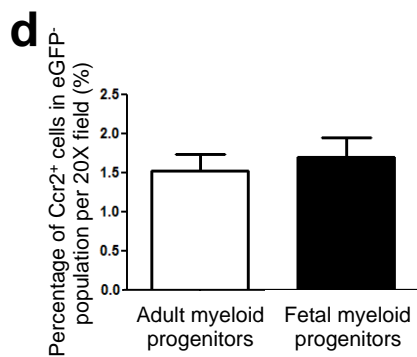
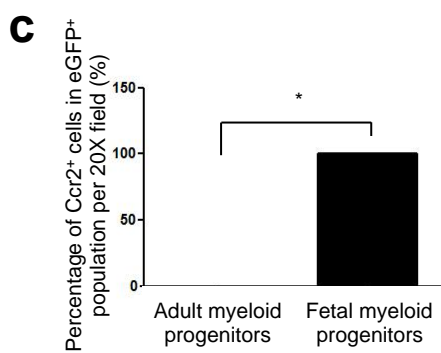
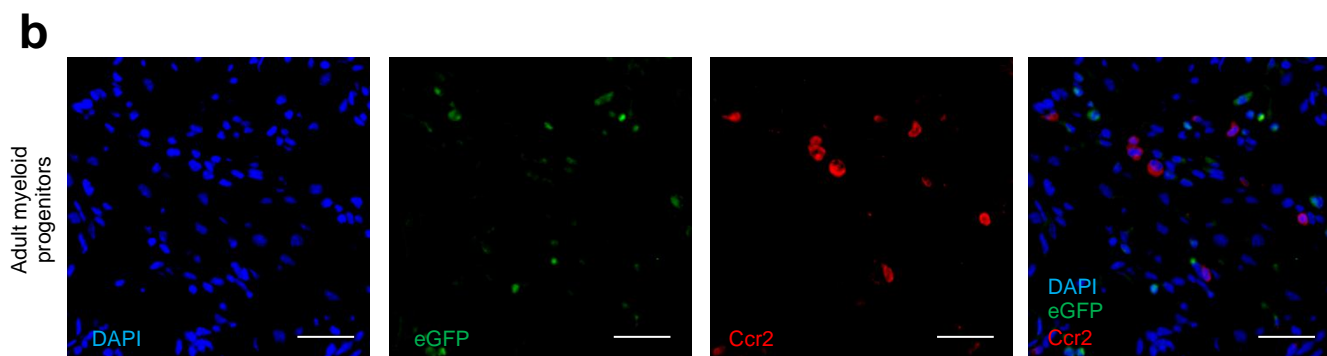
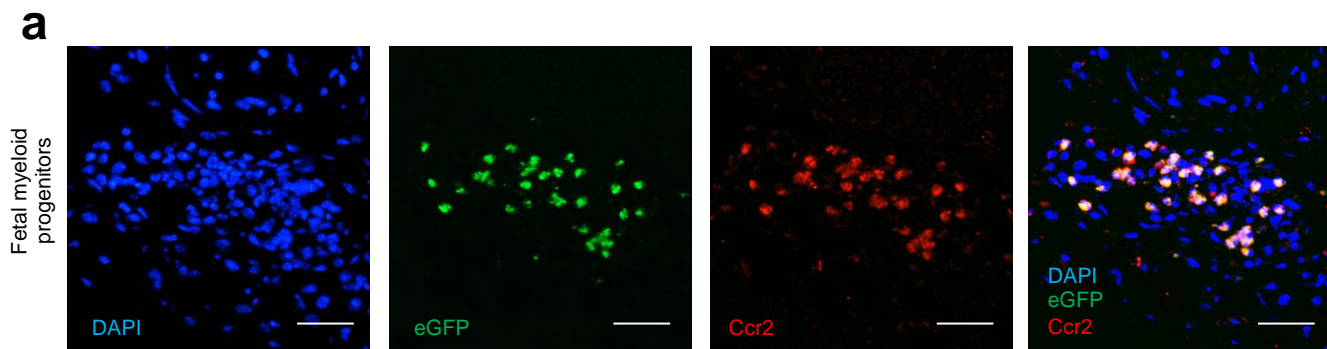
Supplementary Figure 10: Ccl2 has no effect on recruiting fetal EPCs to wound

Peripheral mononuclear blood cells (PBMC) were collected from pregnant female mice carrying eGFP⁺ fetuses or from virgin control mice, with and without wounds, on days 0, 1, 2, 3, for FACS analysis. FACS quantification of CD34/CD31 staining in the CD11b⁻ gate, for virgin mice (**a**), in the eGFP⁻ gate for pregnant mice carrying eGFP⁺ fetuses (**b**), and in the eGFP⁺ gate for pregnant mice carrying eGFP⁺ fetuses (**c**) ($n = 3$). Pregnant female mice carrying eGFP⁺ fetuses were wounded, and PBS or CCL2 was injected into the wound immediately and two days after wounding. PBMCs and wounds were collected seven days after wounding, for FACS analysis. The percentages of CD11b⁻ CD34⁺ CD31⁺ cells in (**d**) PBMCs ($n = 4$) and (**e**) wound tissues ($n = 4$) were analyzed to determine the levels of maternal CD11b⁻ CD34⁺ CD31⁺ EPCs (eGFP⁻ gate) and fetal CD11b⁻ CD34⁺ CD31⁺ EPCs (eGFP⁺ gate) after the administration of PBS or Ccl2. Student's *t*-test, * $p < 0.05$; mean \pm SEM.



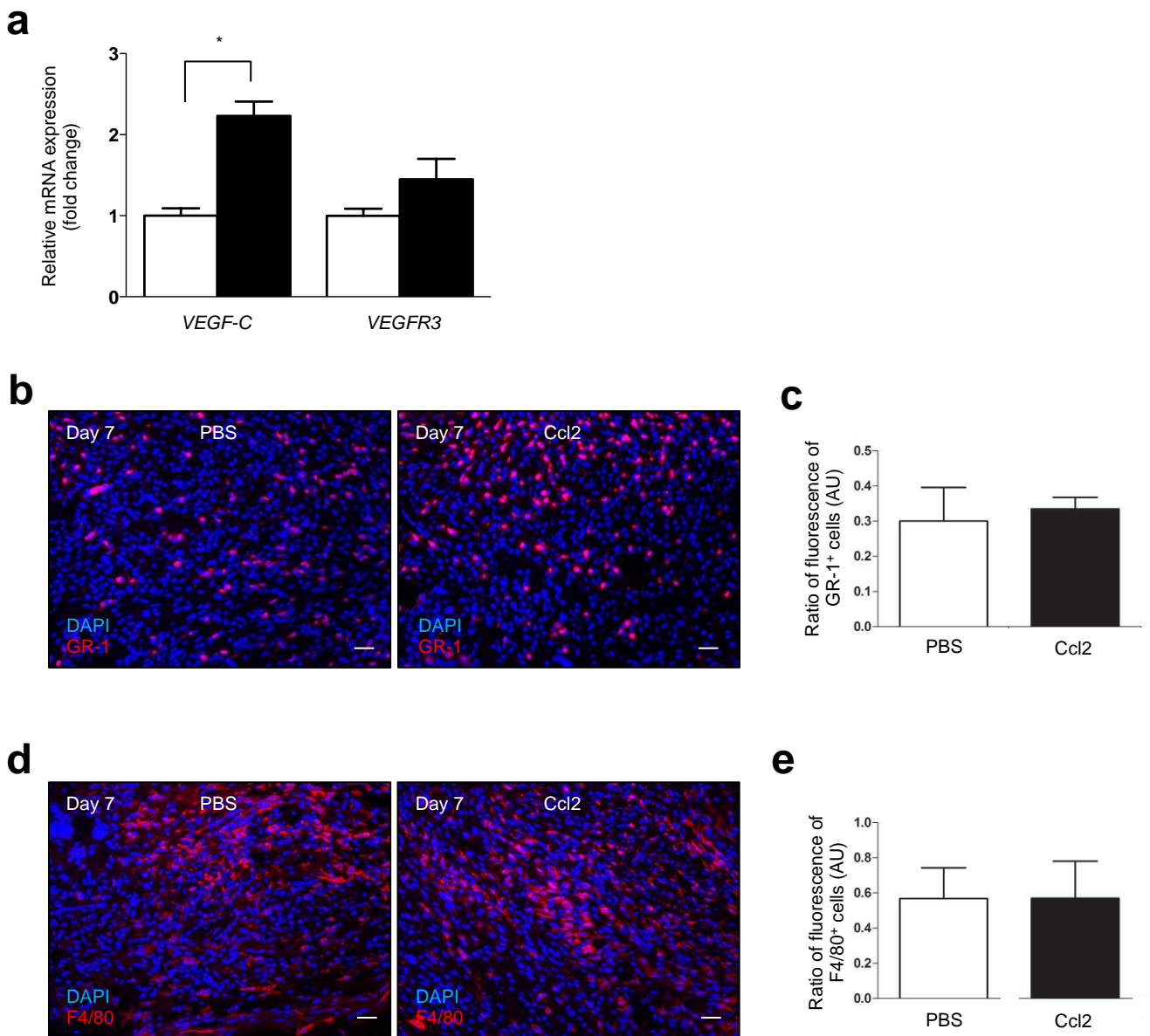
Supplementary Figure 11: Confocal microscopy image of vessels derived from fetal myeloid progenitor cells

Pregnant female mice carrying eGFP⁺ fetuses were wounded and eGFP⁺ CD11b⁺ CD34⁺ CD31⁺ fetal myeloid progenitor cells were isolated from blood on the day after wounding. The recipient mice were normal virgin females with the same genetic background as the donor mice. We transplanted 1×10^5 fetal myeloid progenitor cells into the wound of the recipient mouse on day 1 after wounding, and the wound was harvested on day 7. Confocal analysis of cryosections labeled for vWF (red) and displaying spontaneous eGFP (green) fluorescence. Scale bars: 50 μ m



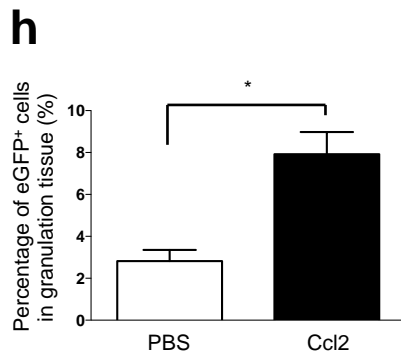
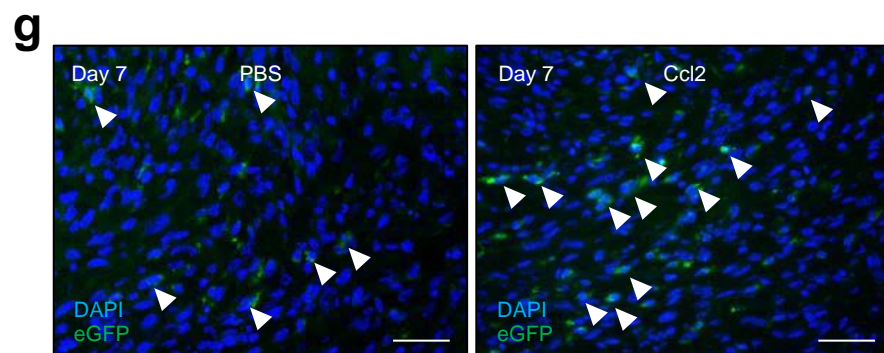
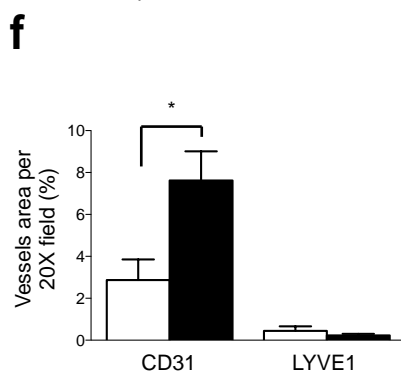
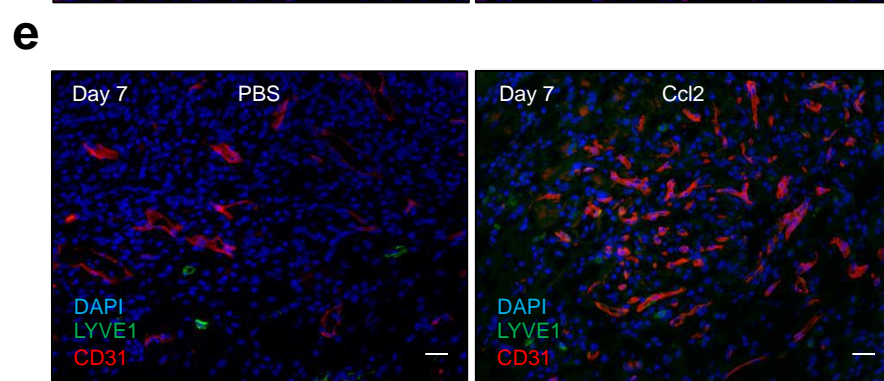
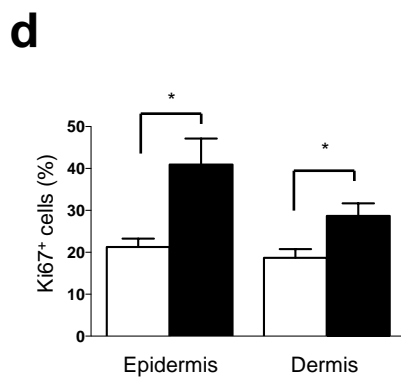
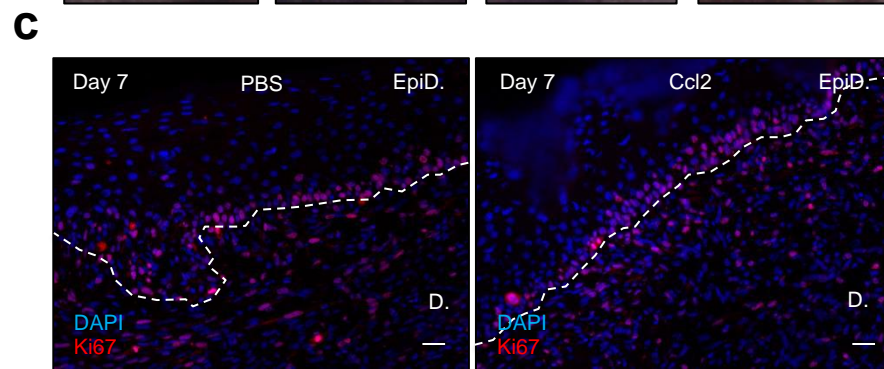
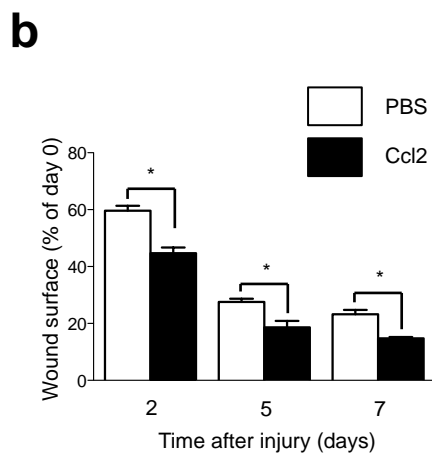
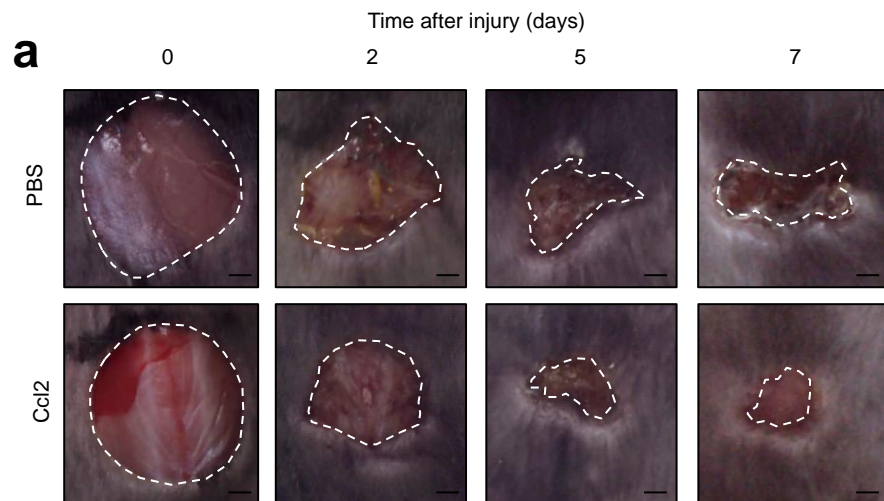
Supplementary Figure 12: A large percentage of fetal myeloid progenitor cells produce Ccr2 after maternal skin injury

Pregnant female mice carrying eGFP⁺ fetuses were wounded and eGFP⁺ CD11b⁺ CD34⁺ CD31⁺ fetal myeloid progenitor cells were isolated from blood on the day after wounding. Alternatively, CaG-eGFP mice were wounded and eGFP⁺ CD11b⁺ CD34⁺ CD31⁺ myeloid progenitor cells were isolated from blood on the day after wounding. The recipient mice were normal virgin females with the same genetic background as the donor mice. We transplanted 1×10^4 fetal myeloid progenitor cells or myeloid progenitor cells into the wound of the recipient mouse on day 1 and the wound was harvested on day 7. Cryosections of **(a)** fetal myeloid progenitor cells with anti-Ccr2 (red) labeling and **(b)** adult myeloid progenitor cells with anti-Ccr2 (red) labeling and spontaneous eGFP (green) fluorescence. Scale bars: 50 μ m. **(c)** Quantification of Ccr2⁺/eGFP⁺ cells among transplanted fetal myeloid progenitor cells or adult myeloid progenitor cells. **(d)** Quantification of Ccr2⁺/eGFP⁻ cells among transplanted fetal myeloid progenitor cells or adult myeloid progenitor cells. **(e)** Representative FACS analysis of blood from pregnant mice carrying eGFP⁺ fetuses on day 1 after wounding, with gating for CD11b⁺ CD34⁺ CD31⁺ eGFP \pm cells. **(f)** Quantification of Ccr2⁺ cells in the CD11b⁺ CD34⁺ CD31⁺ eGFP \pm gate ($n = 3$).



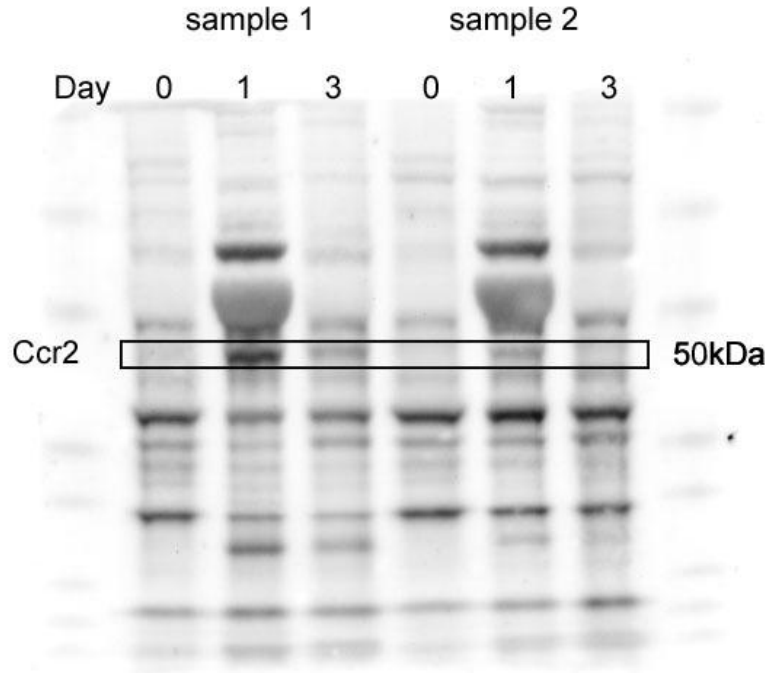
Supplementary Figure 13: Ccl2 administration does not affect inflammation during delayed wound healing in a postpartum model

Each mouse received 12 daily topical applications of dermoval cream after the delivery. An 8 mm wound was created on the clobetasol-treated skin of female mice after delivery (they had carried eGFP⁺ fetuses) and we injected PBS or Ccl2 into the lesion immediately and two days after skin excision. **(a)** Quantitative RT-PCR analysis of *VEGF-C* and *VEGFR3* mRNA levels normalized against *Gapdh* mRNA levels in the wound on day 7 ($n = 3$). **(b)** Anti-GR-1 (red) labeling of the wound. Scale bars: 50 μ m. **(c)** Quantification of GR-1⁺ cells by fluorescence densitometry in granulation tissue ($n = 3$). **(d)** Anti-F4/80 (red) labeling in the wound. Scale bars: 50 μ m. **(e)** Quantification of F4/80⁺ cells by fluorescence densitometry in granulation tissue ($n = 3$).



Supplementary Figure 14: Ccl2 improves delayed wound healing in late postpartum conditions, by recruiting FMCs

Each mouse received 10 daily topical applications of dermoval cream 6 months after the delivery. An 8 mm wound was created on the clobetasol-treated skin of the female mice postpartum (these mice had carried eGFP⁺ fetuses) and we injected PBS or Ccl2 into the lesion immediately and two days after skin excision. **(a)** Time course analysis of the healing of the excisional skin lesion; a representative image is shown. Scale bars: 1mm. **(b)** Planimetry of the wound area relative to the initial wound area, at each time point ($n = 3$). **(c)** Anti-Ki67 (red) labeling of the wound. Scale bars: 50 μ m. **(d)** Quantification of Ki67⁺ cells in epidermal wound edges (EpiD) and the dermal granulation tissues (D) ($n = 3$). **(E)** Dual labeling for CD31 (red) and LYVE1 (green). Scale bars: 50 μ m. **(f)** Quantification of relative vessel area per 20x field by fluorescence densitometry ($n = 3$). **(g)** Wound sections from pregnant mice carrying eGFP⁺ fetuses, after the injection of PBS or Ccl2. Representative micrographs of the spontaneous fluorescence of eGFP⁺ (green) cells in granulation tissue, indicated by white arrowheads. Scale bars: 50 μ m. **(h)** Quantification of eGFP⁺ cells in sections of wounds from pregnant mice carrying eGFP⁺ fetuses after the injection of PBS or Ccl2 ($n = 3$). Student's *t*-test, * $p < 0.05$; mean \pm SEM.



Supplementary Figure 15: Full Ccr2 Western Blot membrane

Wound samples were homogenized in RIPA buffer supplemented with Complete Protease Inhibitor Cocktail and centrifuged to obtain lysates. Equal amounts of extracted protein (20 μ g) were subjected to SDS-PAGE in a NuPAGE 4-12% Bis-Tris Gel and transferred to nitrocellulose membranes.

	PBS (n = 4)	CCL2 (n = 4)
WBC (10 ³ /mm ³)	5.15 ± 0.93	4.20 ± 1.06
LYM (10 ³ /mm ³)	3.90 ± 0.63	3.25 ± 0.75
MON (10 ³ /mm ³)	0.12 ± 0.09	0.05 ± 0.05
GRA (10 ³ /mm ³)	1.12 ± 0.22	0.90 ± 0.27
EOS (10 ³ /mm ³)	0.18 ± 0.02	0.21 ± 0.04
RBC (10 ⁶ /mm ³)	6.51 ± 0.32	6.52 ± 1.10
HGB (g/dL)	12.65 ± 0.46	12.45 ± 1.53
HCT (%)	29.72 ± 1.57	29.75 ± 5.12
MCV (µm ³)	45.50 ± 0.57	45.75 ± 0.50
MCH (pg)	19.40 ± 0.39	19.20 ± 1.03
MCHC (g/dL)	42.50 ± 0.99	42.15 ± 2.41
RDW (%)	14.85 ± 0.26	15.07 ± 0.33
PLT (10 ³ /mm ³)	1437.50 ± 138.09	1318.25 ± 199.29
MPV (µm ³)	5.55 ± 0.12	5.45 ± 0.10
Glucose (mg/dL)	192.25 ± 20.41	172.50 ± 27.74
GGT (U/L)	<5,00	<5,00
Creatinin (mg/dL)	<0,50	<0,50

Supplementary Table 1: Ccl2 injection into wound tissue has no effect on blood cell counts, glycemia, GGT and creatinine levels